

Article

Rice Husk Ash Incorporation in Calcium Aluminate Cement Concrete: Life Cycle Assessment, Hydration and Strength Development

Amirmohamad Abolhasani ¹ , Bijan Samali ^{2,*} and Fatemeh Aslani ¹

¹ Department of Civil Engineering, Babol Noshirvani University of Technology, Babol 47148-71167, Iran; amirmabolhasani@nit.ac.ir (A.A.); fatemeh.aslani.gh@nit.ac.ir (F.A.)

² Centre for Infrastructure Engineering, School of Engineering, Design and Built Environment, Western Sydney University, Sydney 47360263, Australia

* Correspondence: b.samali@westernsydney.edu.au

Abstract: In this research effect of rice husk ash (RHA), as silicate impurities, on the hydration reaction and mechanical strength of calcium aluminate cement (CAC) concrete, as one of the most important non-Portland cements, was investigated. Furthermore, in order to evaluate the environmental performance of mixtures, a lifecycle assessment was performed using the recipe midpoint and endpoint method. Compressive and tensile strength tests were conducted at the ages of 7, 28, and 90 days on specimens containing different contents of RHA (0, 2.5, 5, 7.5, and 10%) substituting for cement at the water-cement ratio of 0.4. Moreover, in order to calculate the hydration reaction of the specimens, thermogravimetric analysis (TGA) was performed at a rate of 10 °C/min to up to 1000 °C. The results revealed that the use of rice husk ash as a partial replacement at a concentration of 5% could reduce CO₂ emission and ozone depletion by 18.75% and 31%, respectively. The findings indicate that, at 90 days, the mechanical strength of the mixes containing RHA were higher than those of the control mix, with the maximum improvement occurring at the substitution percentage of 5%. In accordance with TGA analysis the substitution of 5% RHA in CAC concrete led to a higher hydration level, which in turn improved the mechanical properties relative to the specimen without RHA at 90 days.

Keywords: rice husk ash; calcium aluminate cement; life cycle assessment; mechanical property; hydration reaction



Citation: Abolhasani, A.; Samali, B.; Aslani, F. Rice Husk Ash Incorporation in Calcium Aluminate Cement Concrete: Life Cycle Assessment, Hydration and Strength Development. *Sustainability* **2022**, *14*, 1012. <https://doi.org/10.3390/su14021012>

Academic Editor:
Syed Minhaj Saleem Kazmi

Received: 16 November 2021

Accepted: 6 January 2022

Published: 17 January 2022

Publisher's Note: MDPI stays neutral with regard to jurisdictional claims in published maps and institutional affiliations.



Copyright: © 2022 by the authors. Licensee MDPI, Basel, Switzerland. This article is an open access article distributed under the terms and conditions of the Creative Commons Attribution (CC BY) license (<https://creativecommons.org/licenses/by/4.0/>).

1. Introduction

Calcium aluminate cement (CAC) is employed as the main binding agent in the cementitious matrix to produce a High-Performance Concrete (HPC) type known as Calcium aluminate cement concrete (CACC) [1–5]. Moreover, CAC and ordinary Portland cement (OPC) have different chemical compositions, in that the alumina content of CAC is greater and its silica content is lower than those of OPC. CAC has superior features such as a fast development of strength and high resistance to fire, leading to applications in places where refractoriness and resistance to chemical attack are required [6–8]. Hence, one effective way to improve fire-resistance is to use CAC. Multiple factors such as the concrete constituent features, exposure duration and temperature, and cooling manner affect the concrete performance when exposed to heat. The literature shows the reduction of the concrete mechanical features with the temperature rise. As reported in a paper addressing the post-fire performance of CACC, the decline that occurred in the strength was less than that of the normal OPC concrete; this observation was ascribed to the existence of alumina phases as a binder [9]. On the other hand, CAC hydration compounds, CAH₁₀ and C₂AH₈, are strongly affected by the temperature, such that, the conversion of these compounds into

the more stable phases of C_3AH_6 and AH_3 occur at room temperature, leading to increased porosity and decreased strength [10,11].

Rice husk (RH), the outer shell of rice grains removed during the milling procedure, is a major agricultural byproduct and accounts for around 20% of the 500 million tons of paddy produced worldwide each year [12]. Currently, RH has no wide application, and except for a fraction of it that is consumed as a low-grade fuel in and low-pressure steam generation brick kilns, most of it is often disposed into waterways, leading to their contamination and pollution. Based on research, the rice plant absorbs orthosilicic acid from groundwater and polymerizes it to synthesize amorphous silica in the husk [13,14]. The pozzolanic activity of RHA mainly stems from amorphous silica. The controlled burning of rice husk, RHA with an amorphous silica weight percentage of around 85–95% can be obtained [15,16].

As reported by Henry and Lyman [17], if the energy and heat generated from burning rice husk is employed to dry rice grains in the cyclonic furnace, the production of RHA can fulfill sustainable development goals. The high silica content of RHA makes it a highly reactive pozzolanic material suitable for making lime-pozzolan mixes and replacing Portland cement [18,19]. Another reason for the high reactivity of RHA is the large specific surface area of its particles provided by the porous structure [20]. Replacing cement with RHA leads to the faster early hydration of C_3S , which results from the large specific surface area of RHA particles [21].

Since the life cycle idea was implemented in the engineering field, attempts have been made to use more sustainable and greener concrete ingredients than existing ones via consuming less cement and adding recycled ingredients [22]. As reported in many papers, natural pozzolans can replace OPC in various applications given superior features they provide such as decreased heat evolution, permeability, and costs [23,24]. On the other hand, cement, as the main concrete production material, has the largest share of greenhouse gas (GHG) emissions and energy consumption of the concrete industry. Sustainable development partially solves this problem by employing supplementary cementitious materials (SCMs). The previous research of the authors considered RHA as a silicate impurity and reported that replacing of cement with RHA can improve the mechanical and fracture features of CACC [25–28]. It is thus found that by increasing the silica content in this concrete, the strength can increase.

Several studies have been conducted on the effect of using different pozzolans instead of cement in concrete on the mitigation of CO_2 emissions and other environmental indices, such as fly ash, slag, and volcanic ash [29–31]. Considering the positive effect of RHA, as a rich source of amorphous silica, on the mechanical features of various concrete types, as reported in different studies, the main objective of this study is to address the environmental effects of using this pozzolan in concrete as a replacement for cement. The impact of adding RHA on reducing CO_2 emissions and other environmental indices has not been accurately evaluated in the literature. Thus, with respect to the eco-friendly nature of RHA and the scarcity of data in the literature on the life cycle assessment (LCA) of concrete specimens with RHA, this work conducted LCA (in a geographical region of Iran) and testing the specimens to examine the environmental impact of the concrete mixes. Given the importance of the hydration reaction and curing time in concretes containing pozzolans, this research addressed the hydration reaction level of CACC mixes containing RHA using the thermal gravimetric analysis (TGA) at the age of 90 days and the mechanical features, such as the compressive and tensile strengths, of these mixes at different curing ages (7, 28, and 90 days). In this regard, considering the superior mechanical features of CACC at W/C of 0.4, this ratio was selected as the control to allow for a better aspect of the effect of replacing CAC with impure silica (at weight percentages of 2.5, 5, 7.5, and 10%) at different ages.

In addition, the obtained findings were compared with the corresponding findings reported in the literature for other types of concrete to evaluate the behavior of this concrete with RHA against that of concretes with various other pozzolans.

2. Materials and Methods

2.1. Materials and Mixture Proportions

This study employed Fondo refractory cement (IR-40) produced by Iran Refractory Cement Plant with a specific gravity of 2.98. It was partially replaced by RHA with a specific gravity of 2.32. The production process of RHA included the burning of rice husk produced in northern Iran at around 700 °C at a heating rate of 10 °C/min based on [32]. For an hour, rice husk was exposed to the target temperature to produce RHA, which was then received a fast cooling of less than 5 min to reach the ambient temperature after removal from the furnace. RHA was cooled down quickly mainly for the formation of non-crystalline silicate and not non-reactive crystalline silicate [32]. X-ray fluorescence (XRF) method was employed to obtain the physicochemical features of RHA and CAC, as can be seen in Table 1.

Table 1. The Results of XRF Analysis of the Calcium aluminate cement and RHA.

Oxide Composition (%)	SiO ₂	Al ₂ O ₃	Fe ₂ O ₃	MgO	CaO	P ₂ O ₅	Na ₂ O	K ₂ O	MnO	Ig. Loss	Blaine Surface Area	Specific Gravity
RHA	90.11	1.19	0.848	0.897	0.89	0.861	-	3.84	0.099	4.05	3600	2.32
CAC	5.25	38.22	13.87	0.97	37.49	0.089	0.311	0.072	0.078	1.04	2900	2.98

Figure 1 presents the XRD patterns for RHA samples. With respect to the peak amorphous range of SiO₂, peak RHA values are in the 2 θ range. Hence, when RHA is burnt at around 700 °C, as a relatively elevated temperature, silica experiences amorphous crystallization, in which the chance of any crystalline reflection is small. Papers [33] and [34] reported spectra similar to this spectrum. Figure 2 gives the XRD patterns for CAC, in which the primary phase is CA, followed by small quantities of C2AS and CT. The coarse and fine particles employed here had the saturated surface dry (SSD) condition. For the coarse particles, max. particle diameter = 12 mm, specific gravity = 2.5, and water-absorbing percentage = 0.5%, while for the fine particles (washed river sand), fineness modulus = 2.61, specific gravity = 2.6, and water-absorbing percentage = 0.7%. Running water was poured in the mixes.

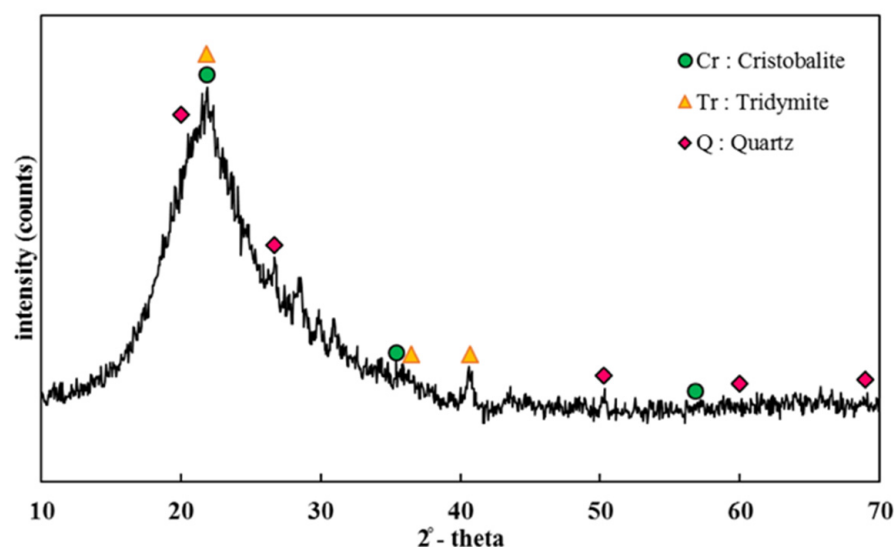


Figure 1. XRD pattern of rice husk ash.

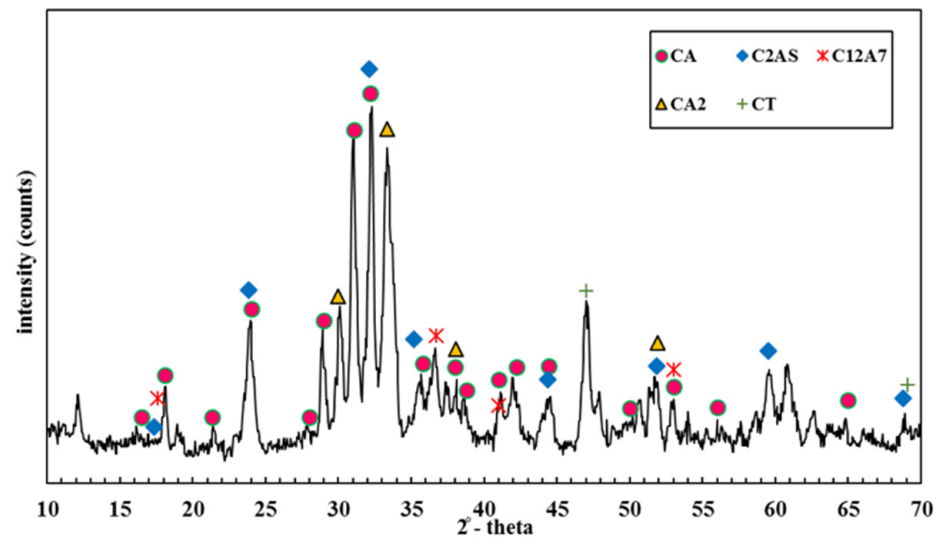


Figure 2. XRD pattern of calcium aluminate cement.

The mix proportion of CACC is shown in Table 2. The sieve test was carried out on the fine and coarse particles to determine their size distribution graphs, as shown in Figure 3. It is seen that these graphs are consistent with the standard range of ASTM C33 [35]. The workability of the mixes was improved by a poly-carboxylate ether-based high-performance superplasticizer (specific gravity = 1.11). Based on the previous papers of the authors, $W/C = 0.4$ provided the best mechanical features for CACC compared with other W/C s [25]; thus, the concrete mixes were produced with this W/C and partial cement replacement of 0 and 5% by RHA in different curing age, such as 7, 28, and 90 days.

Table 2. Mix proportion of CAC mixtures with different RHA partial replacements to cement.

Mix Number	Mix Name	RHA (kg/m ³)	Cement (kg/m ³)	Water (kg/m ³)	Coarse Aggregate (kg/m ³)	Fine Aggregate (kg/m ³)	SP (kg/m ³), (SP/Binder)	Slump (mm)
Mix1	CAC-RHA0-0.4	-	450	180	840	905	0.378 (0.08%)	100
Mix2	CAC-RHA2.5-0.4	11.25	438.75	180	840	905	0.756 (0.16%)	95
Mix3	CAC-RHA5-0.4	22.5	427.5	180	840	905	1.512 (0.33%)	80
Mix4	CAC-RHA7.5-0.4	33.75	416.25	180	840	905	2.646 (0.58%)	60
Mix5	CAC-RHA10-0.4	45	405	180	840	905	2.989 (0.66%)	60

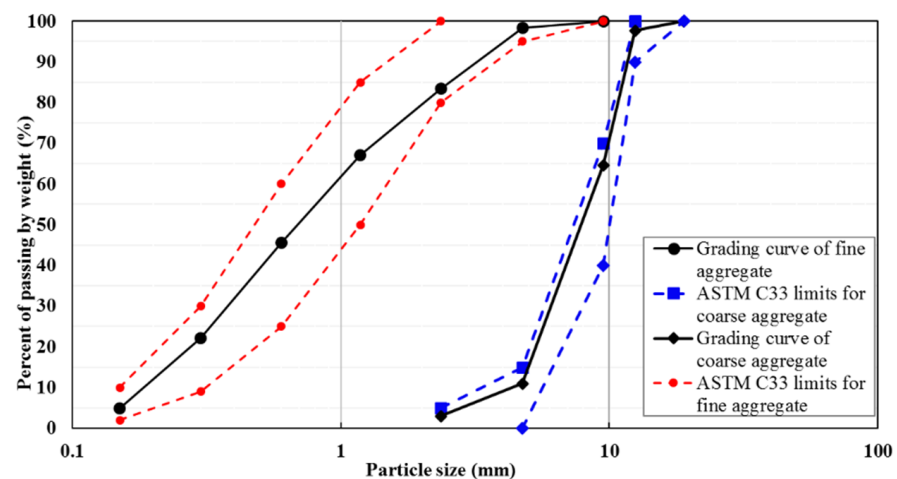


Figure 3. Gradation curves of fine and coarse aggregates.

2.2. Manufacturing and Testing Specimens

Mechanical and Microstructural Tests

Following the removal of the molds, the curing of the specimens was conducted at temperature = 20 ± 5 °C and relative humidity = 75% for 28 days. For assessing the compressive capacity, based on the recommendations of BS-EN123090 [36], three $100 \times 100 \times 100$ mm cube specimens were manufactured from each mix. Additionally, ASTM C496 [37] recommendations were followed to manufacture three 300×100 mm (height \times diameter) cylinder specimens. As can be seen in Figure 4, After weighing the three concrete cubes and the three concrete cylinders made from each mix, they were subjected to compression and tension tests. Although BS-EN123090 specifies a loading rate range of 0.6 ± 0.2 MPa/s for the compression test, in this work, a loading rate of 0.25 MPa/s was selected for this test. Also, ASTM C496 specifies a loading rate range of 0.14–0.7 MPa/sec for the splitting tension test on concrete cylinders; thus, a loading rate of 0.51 MPa/sec was considered here for this test. To determine the mineralogy of materials, XRD analysis was conducted in PW1730 using Cu K α radiation and scanning unprinted powder solids in the $2\theta = 5$ – 80° range with 0.05 dig step interval and scanning rate of 0.1 deg. s⁻¹. The kinetics and performance of the CACC for exposure temperatures ranging from the ambient temperature to 1000 °C were investigated by the thermogravimetric analysis (TGA) conducted at a fixed heating rate of 10 °C/min with a TA-Q600 device in vacuum atmosphere (zero air).



Figure 4. Tests of hardened concrete.

2.3. LCA Methodology

2.3.1. Environmental Impact Assessment

Life-cycle assessment (LCA) is a method used for assessing the impact of resources, environment, and system health (production process, product, or services). In this case, net system is a process needed to present a specific product, which can be used to better understand the whole system used for producing a certain product and thus to improve it (Jorgensen et al.). Zobel et al. [38] proposed the use of LCA method based on ISO 14040 and ISO/WD 14042 and in the documentation format based on ISO 14048 as a method for determining the main environmental aspects [39]. In this study, LCA was conducted based on guidelines stated to evaluate the environmental effects of the partial replacement of cement with RHA in CACC. The following stages are the main aspects of methodology, assumptions, and materials in the LCA.

- (a) Goal and scope definition
- (b) Inventory analysis
- (c) Environmental impact assessment and interpretation phase

2.3.2. Goal and Scope

The initial step is the goal and scope definition, which specifies the scope of study. The main goal of this study in this step is to determine and compare the environmental effects of the partial replacement of cement with RHA in concrete production. The motivation for this choice was the knowledge of the authors of the fact that the most important stage in terms of environmental impacts is the production stage, as mentioned by several researchers [40–42]. In this study, the Simapro v.9 was used for evaluation.

This research aimed at establishing the life cycle steps from cradle to gate since there are many potential applications for mixture design in different structural elements. According to ISO 21930, if the performance of a product, as a construction material, is not clear for all its life cycle, a clarified unit is used [43]. The performance unit was considered per each cubic meter of the concrete mix, and also the amount of material in each design was put as the input weight unit in the software. For example, cement was entered in kg. The unit of concrete was selected as m³, and the replacement percentages of RHA ranged from 0 to 10%. Note that in the conducted LCA, environmental impacts related to in-situ material placement (construction), repair and replacement over time, maintenance scenarios, and service life termination are not included in this research.

2.3.3. Inventory Analysis

Here, in the Simapro software, the databases of Ecoinvent v.3.4 and Agri-footprint were used. With more than 10,000 datasets in various areas, Eco invent is the most comprehensive international LCI for calculating LCA [44]. In this stage of LCA, all the inputs and outputs of the life cycle stages were considered. In addition, required input energies and data were extracted from Chungsangunsit et al. [45] and Wang et. al. [46]. RHA was considered as the final output, and according to previous studies [20,25,32,34], it was used in concrete as a partial replacement of cement. A list of all inventories used here can be seen in Table 3. The emissions produced from the production of all the concrete constituents are included in the analysis.

Table 3. Inventory data available for rice husk ash concrete (1 cum) [38,39].

Input/output	Unit	Value
Cement	kg	Based on mix designs
Sand	kg	840
Crushed Gravel	kg	905
Water	kg	180
Superplasticizer	kg	Based on mix designs
Materials and Energy used for processing of Rice husk ash		
Electricity	MJ	6.30×10^1
Rice husk	kg	2.43×10^2
Carbon dioxide	kg	3.36×10^2
Carbon monoxide	kg	5.90×10^0
Nitrogen dioxide	kg	6.39×10^{-1}
Methane	kg	1.94×10^0
Dust (PM 2.5)	kg	1.94×10^0
Rice Husk Ash	kg	4.92×10^1
RHA transportation	kJ/kg	3.8 (distance 32 km)

3. Results

3.1. Hydration Process of 90-Day Paste

The thermal performance of the CACC for exposure temperatures of the ambient temperature to 1000 °C was obtained using the TGA performed at a fixed heating rate of 10 °C/min in vacuum (zero air) with a TA-Q600 device. In Figure 5a, the production level of C-S-H gel can be seen based on the shown TGA results for both designs at 90 days of age. It is seen that both curves drop considerably at two points, this first of which occurs at

temperatures of 150 to 300 °C as a result of the dehydration of multiple hydrates, mostly C-S-H. The other point corresponds to a significant mass loss at temperatures of 650 to 850 °C, which is attributed to the decomposition decarbonation and of calcium carbonate.

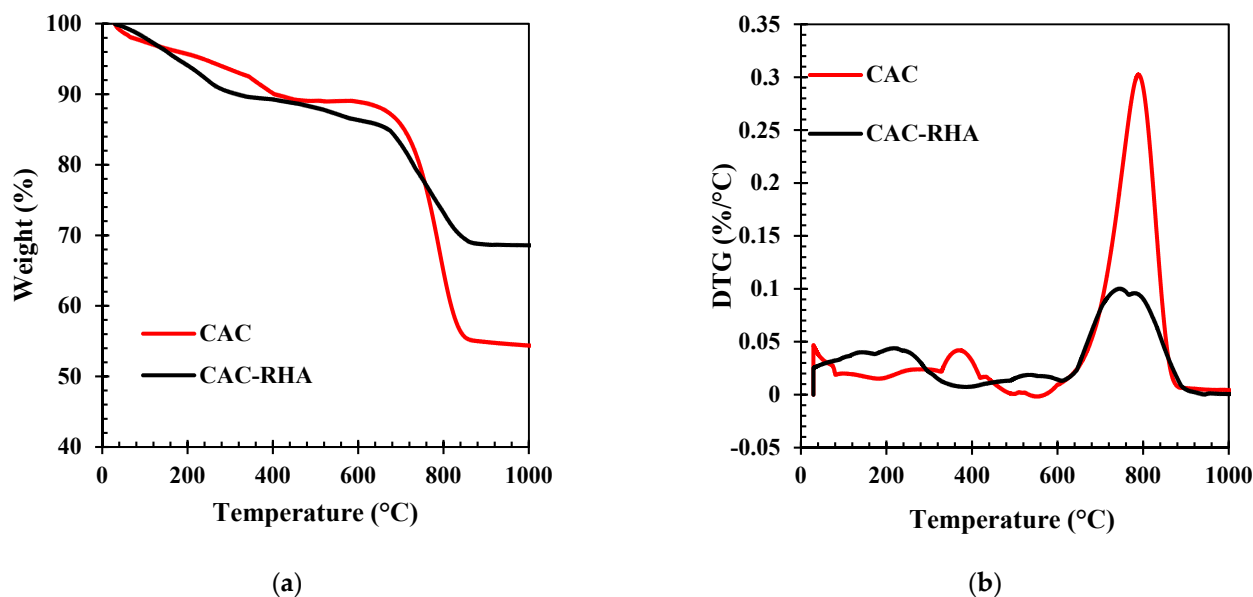


Figure 5. (a) TGA and (b) DTG graphs of concretes containing CACC and CAC-RHA.

Another paper addressing the hydration level of normal OPC concrete containing RHA [47] reported another drop at temperatures 450 to 550 °C besides the mentioned two drops; this other drop was reported to result from the portlandite (another hydration product) dihydroxylation. Due to a low portlandite content of CACC, this drop in the above temperature range was smaller in this concrete relative to normal concrete. Nevertheless, concretes with RHA experienced a relative drop in this range; this indicates that incorporating pozzolanic materials raises the cement matrix activity and speeds up the secondary hydration of $\text{Ca}(\text{OH})_2$. According to the above discussion, the structure of pozzolans leads to the continuation of their hydration even more than 28 days, with moisture in the porosity giving rise to hydration compounds. As previously mentioned, the C-S-H gel dehydration at temperatures between 150 and 300 °C leads to a mass loss. These findings can serve as direct indicators of the RHA reactivity level and obtain the concrete's hydration level.

In the above temperature range, the concretes with RHA have higher mass losses than those without RHA, as shown in Figure 5b. Thus, at 90 days, adding 5% RHA in CACC increased the level of hydration and consequently yielded better mechanical features than those of the concrete without RHA. Moreover, the mass loss of the concrete without RHA was higher after exposure to 650 °C. It is seen that the concrete with RHA is more durable and deteriorates less when exposed to high temperatures of up to 1000 °C.

3.2. Hardened CACC Features

3.2.1. Compressive Strength

The reported compressive capacity is the mean compressive capacity of three identical 100-mm cubes. In Table 4, the compressive capacity values of CACC specimens at different W/Cs are provided. With the rise in W/C, the compressive capacity decreases, as similarly reported by Padhi [48]. At W/C = 0.4, the highest compressive capacity occurred. Further, raising W/C from 0.4 to 0.45, 0.5 and 0.55 lowered the compressive capacity by 12.7, 39, and 55%, which can result from the inverse relationship of the compressive capacity and pore volume. Thus, higher W/Cs led to further compressive capacity decline as a result of higher porosity in the concrete microstructure due to the escaping of free water not participating in hydration, in turn lowering the maximum compressive capacity [49]. The 7-, 28-, and 90-day compressive capacity values of CACCs with different RHA percentages

substituting for cement is listed in Figure 5. As can be seen, the 7- and 28-day concretes with RHA show declining compressive capacity trends. In this regard, Madandoust et al. [34] reported that the short-term capacity of the specimen with RHA was smaller than that of conventional concrete. It is also seen that the 7-day capacities of the concretes with 2.5, 5, 7.5, and 10% RHA declined by 8, 16, 27, and 32%, respectively, compared with that of the concrete without RHA.

Table 4. Compressive Strength of Calcium aluminate cement concrete with different RHA partial replacements at different ages.

Mix Design	Average Compressive Strength-7 Days (COV)	Average Compressive Strength-28 Days (COV)	Average Compressive Strength-90 Days (COV)
CAC-R0-0.4	67.6 MPa ($\pm 2.31\%$)	82.5 MPa ($\pm 2.86\%$)	85.8 MPa ($\pm 2.49\%$)
CAC-R2.5-0.4	61.73 MPa ($\pm 3.96\%$)	77.47 MPa ($\pm 4.05\%$)	87.24 MPa ($\pm 3.8\%$)
CAC-R5-0.4	56.4 MPa ($\pm 2.05\%$)	73.38 MPa ($\pm 2.33\%$)	90.13 MPa ($\pm 2.88\%$)
CAC-R7.5-0.4	49.21 MPa ($\pm 2.38\%$)	64.82 MPa ($\pm 1.45\%$)	88.65 MPa ($\pm 5.41\%$)
CAC-R10-0.4	46.1 MPa ($\pm 2.67\%$)	62.43 MPa ($\pm 1.49\%$)	84.32 MPa ($\pm 3.15\%$)

According to Table 4, at the age of 28 days, the compressive capacities declined by 6, 11, 21, and 24% in the presence of respectively 2.5, 5, 7.5, and 10% RHA. When RHA is present in the concrete mix, it initially absorbs a notable volume of water, in turn limiting the amount of water available for the cement hydration [50]. Various factors including the W/C, curing regime, and the mix proportions are related to the compressive capacity drop [51]. In the concretes with RHA, the compressive capacity values were considerably higher than those of the control concrete at 90 days of age. In this regard, the specimen with 5% RHA experienced the maximum 90-day compressive capacity, which was around 23% greater than the 28-day compressive capacity of the corresponding concrete. The level of secondary hydration was only about 4%, as expected.

The results showed that as the RHA percentage increased in these concretes, the secondary hydration increased proportionally; this in turn recovered the 28-day strength drop. Noaman et al. [52] observed similar results by incorporating RHA in the brick aggregate concrete. In addition, Salas et al. [53] reported the improved compressive capacity by incorporating 5–10% RHA. Figure 6 shows the compressive capacity variation of the concretes at 7–90 days of age. This figure shows more increase in the strength of the concretes with higher RHA contents at 28–90 days of age, which is ascribed to the secondary hydration in all the specimens with the pozzolan; other paper also reported similar results. It is seen that the strength of the concrete with 5% RHA at 90 days is 23% greater than that at 28 days. Nevertheless, a different trend occurs in the concrete lacking RHA, in which 82% of the 28-day capacity is reached at 7 days, and the strength at 90 days is only 4% greater than that at 28 days; this results from the initial setting and greater initial strength of CACCs.

The greater specific surface area compared with cement and the high reaction tendency of RHA leads to its extensive reaction with the calcium hydroxide generated from the hydration and the production of more C-S-H gel in long term. This produced C-S-H gel increases the compressive capacity through filling voids, reducing porosity, and improving the ITZ in the cement matrix. Based on the results, the incorporation of above 5% RHA lowered the compressive capacity of the concretes at 90 days, which can be due to a large silica content (provided by RHA) accessible for reaction with $\text{Ca}(\text{OH})_2$ formed in early cement hydration. When the hydrated cement structure has a high content of silica, it is highly probable that the amount of C-S-H gel formed is insufficient to react with all the silica available, which in turn leads to the lack of a chemical reaction for a portion of silica. Thus, a considerable part of silica experiences no reaction.

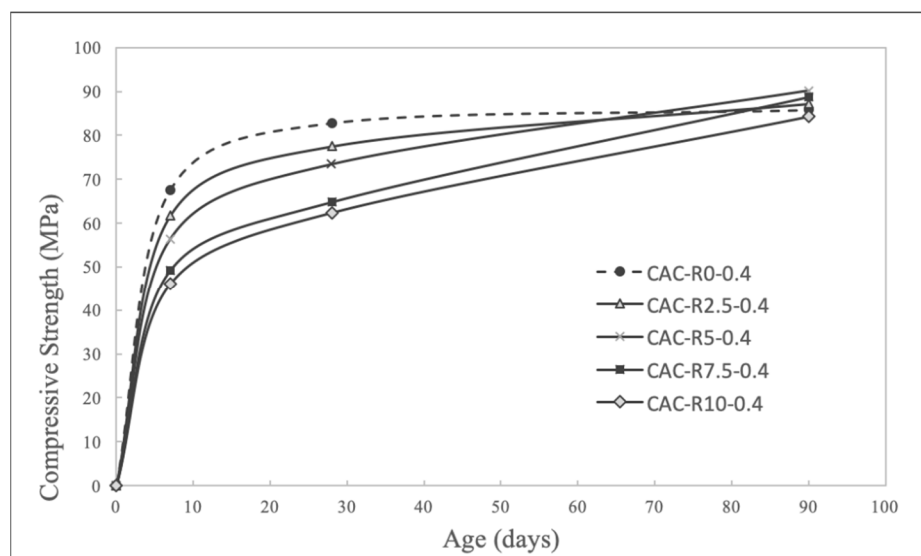


Figure 6. Variation of Compressive strength at different ages with four RHA dosage levels.

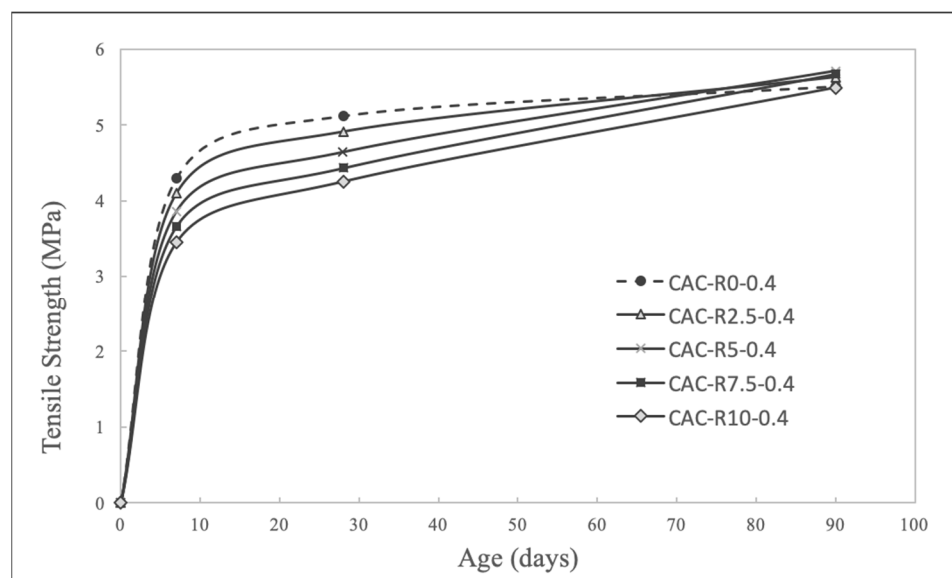
3.2.2. Tensile Strength

The tensile capacity values of the 28-day CACC specimens can be seen in Table 4, according to which, increasing the W/C lowers the tensile capacity. The tensile capacity values of the specimens with W/Cs of 0.45, 0.5, and 0.55 were respectively 18.5, 37, and 50% lower than that of the specimens with a W/C of 0.4. This occurred due to an increase in porosity and a decline in aggregate-cement matrix cohesion by raising W/C. In Figure 6, the ultimate tensile capacities of the 7-, 28-, and 90-day CACC specimens are provided. As Table 3 shows, at an age of 28 days, the addition of RHA lowered the ultimate tensile capacities of 28-day CACC specimens with W/C of 0.4. RHA addition declined the tensile capacity at an age of 7 days. In this regard, the presence of 2.5, 5, 7.5, and 10% RHA led to 4, 10, 15, and 19%, respectively, decline in the tensile strength compared with that of concrete lacking RHA.

According to Table 5, at the 28 days, the tensile capacity values of the specimens with 2.5, 5, 7.5, and 10% RHA declined by 4, 10, 13.5, and 17%, respectively, compared with that of concrete lacking RHA. As discussed about the compressive capacity, this descending trend of tensile capacity occurs as a result of the specific surface area of RHA being larger than that of cement, which leads to the absorption of more water by the mix and the consequent lower 28-day hydration level. As a result of this, more micro cracks form in the ITZ, leading to a reduced tensile capacity [54]. Figure 7 indicates that at 90 days, increasing the RHA percentage recovers the 28-day tensile capacity drop and that the tensile capacity values become even larger than that of the control concrete. The specimen with 5% RHA as a CAC replacement gave rise to the maximum 90-day tensile capacity, being larger than the corresponding value at 28 days by 23%. The 90-day tensile capacities were 14, 28, and 29% larger than the 28-day tensile capacity for the specimens containing 2.5, 7.5, and 10% RHA, respectively. Furthermore, raising the content of RHA from 2.5 to 10% showed that the 28-day strength increased more than the 7-day strength. The XRF analysis indicates that RHA consists of above 90% silica and a small quantity of alumina; hence, with increasing the RHA content, the silica volume of the cementitious mixture increases while its alumina volume decreases. Thus, the 7-day strength is higher than the 28-day strength for the specimens with higher alumina contents due to the formation of a greater quantity of tricalcium aluminate.

Table 5. Tensile Strength of Calcium aluminate cement concrete with different RHA partial replacements at different ages.

Mix Design	Average Tensile Strength-7 Days (COV)	Average Tensile Strength-28 Days (COV)	Average Tensile Strength-90 Days (COV)
CAC-R0-0.4	4.3 MPa ($\pm 2.86\%$)	5.12 MPa ($\pm 3.71\%$)	5.51 MPa ($\pm 2.65\%$)
CAC-R2.5-0.4	4.1 MPa ($\pm 1.84\%$)	4.91 MPa ($\pm 1.01\%$)	5.63 MPa ($\pm 3.86\%$)
CAC-R5-0.4	3.86 MPa ($\pm 2.86\%$)	4.64 MPa ($\pm 3.13\%$)	5.71 MPa ($\pm 3.11\%$)
CAC-R7.5-0.4	3.66 MPa ($\pm 3.18\%$)	4.43 MPa ($\pm 2.9\%$)	5.67 MPa ($\pm 3.9\%$)
CAC-R10-0.4	3.45 MPa ($\pm 2.49\%$)	4.25 MPa ($\pm 1.20\%$)	5.49 MPa ($\pm 2.64\%$)

**Figure 7.** Variation of Splitting Tensile strength at different ages with four RHA dosage levels.

As discussed for the compressive capacity, the tensile capacity at 90 days increases since RHA shows an appropriate performance in the hydration process above 28 days, leading to the formation of more C-S-H gel through reaction with $\text{Ca}(\text{OH})_2$ and the consequent improved CACC microstructure. Christopher et al. [55] reported a similar trend. Furthermore, Noaman et al. [46] reported that the maximum tensile capacity occurred at the W/C of 0.5 in the specimen with 10% RHA. Considering the above, the pozzolanic features of RHA together with its filler role improves the tensile capacity. As effects of the presence of RHA in concrete, the cement matrix-aggregate ITZ improves, and the content of crystalline calcium hydroxide decreases due to the production of more C-S-H gel [56].

4. LCA Findings

4.1. Impact Assessment

In this research, for the midpoint and endpoint effect assessment, the Recipe method was used, which comprises of two impact category sets associated with a set of factors for characterization. The environmental damage classification in the Recipe endpoint method involves ecosystem and resources, human health, and quality. In this method, environmental effects are specified under seven categories, namely Climate Change (Cc) ($\text{kgCO}_2\text{-Eq}$), Agricultural Land Use (Lu) (m^2a), Stratospheric Ozone Depletion (Od) (kg CFC-11-Eq), Human Toxicity (Ht) (kg1,4-DCB-Eq), Particulate matter (kg PM 10-Eq), Water depletion (m^3), and Fossil depletion (Fd) (kg oil-Eq).

4.2. Midpoint Assessment

For all the mixes, almost the same models were employed for concrete production, with the difference being the contents of cement and sand. Here, the entire concrete

production process, ranging from supplying raw materials to disposing concrete, was taken into account. Rice husk is significantly important for the energy, construction and environmental problems considering its high calorific value and potential role as an SCM. Hence, incorporating it in concrete has beneficial impact on concrete. The midpoint analysis evaluated the impact of different production assessments on the environment.

It is observed in Figure 8 that partially replacing cement with RHA substantially affected all parameters with the exception of mineral resource scarcity, marine eco-toxicity, water reduction, and ionizing radiation. CO₂ emission is an important aspect of the environmental impact assessment. Based on the results of analysis, the emission of CO₂ declines by around 38% for mix 5 given the incorporation of RHA in concrete. A significant cause of air pollution and respiratory problems is the emission fine particulate matter, which in this work declined by around 68% for the mix 5. A significant problem for the assessment of the environmental impact in the past has been associated with the ozone layer depletion through the of emission chlorofluorocarbons, with detrimental effects on the environment. Partially replacing RHA leads to an around 60% decline in the depletion level of ozone layer. A large amount of energy originated from fossil fuels is required for the production and processing of raw materials for the concrete industry. Disposing RHA in agricultural soil leads to the congestion of the soil pores and reduces its fertility. Moreover, the ultrafine particles of RHA fills pores in the soil and blocks the entrance of rainwater into aquifers. As the analysis shows, recycling RHA by using it in concrete leads to an around 20% increase in the use of agricultural lands; a result that is significant for developing countries like Iran, where the shortage is agricultural land is rising.

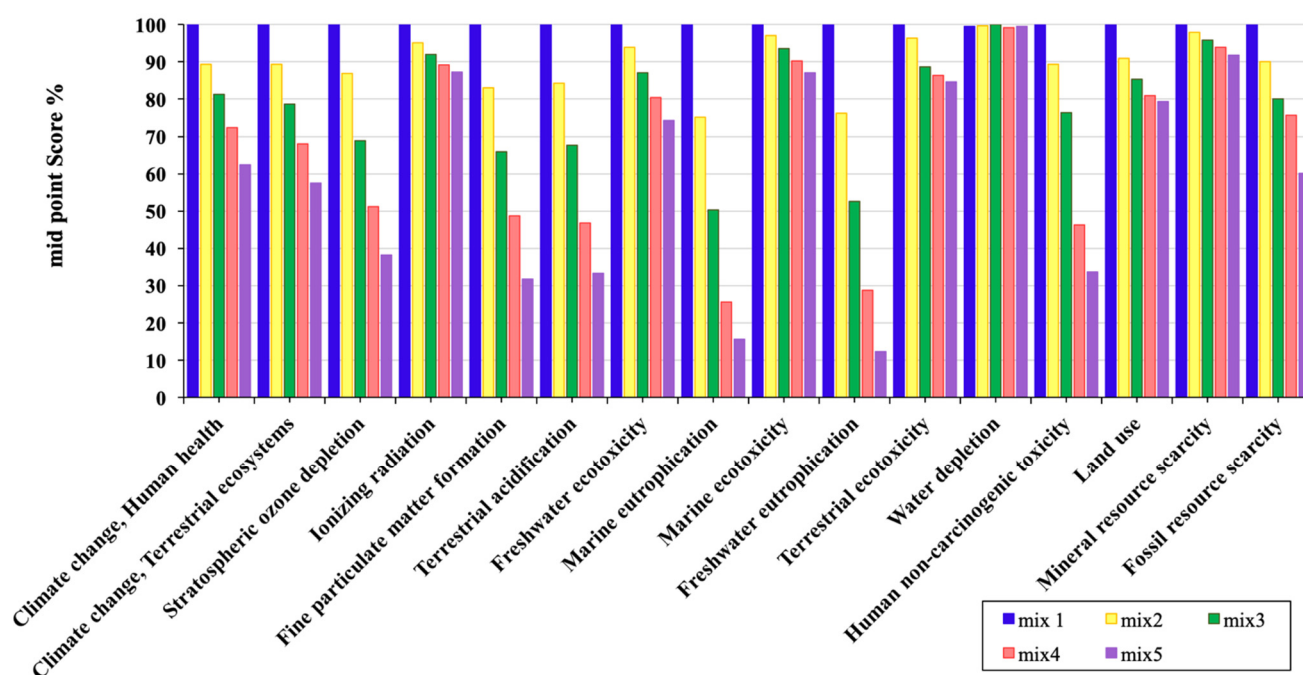


Figure 8. Recipe midpoint analysis results for concrete mixes considered in the analytical study.

4.3. Endpoint Assessment

This assessment deals with the general impact of raw materials on human health, resources, and general ecosystem quality. The results show a clear impact of replacing cement with RHA. As can also be seen, a significant level of electricity is used in cement production. Figure 9 provides results of the endpoint assessment, where parameters with highest impacts are similar with the exception of agricultural land use, eco-toxicity, particulate matter emissions, and terrestrial acidification, which experience a rise.

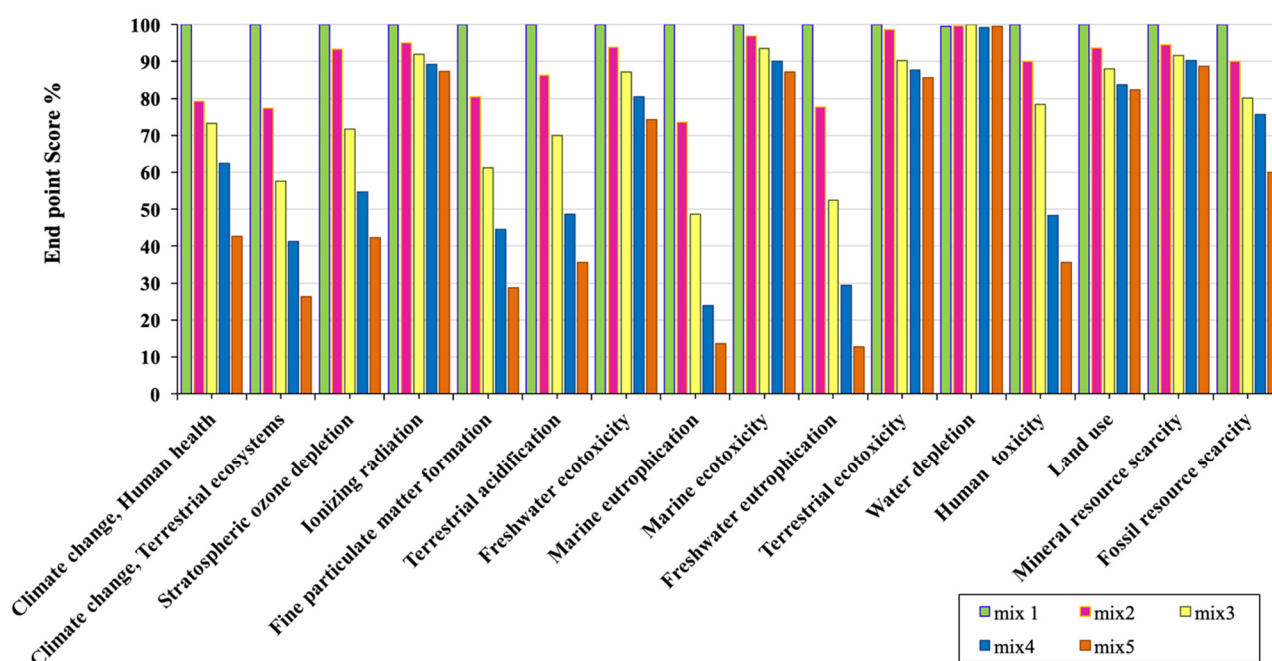


Figure 9. Recipe endpoint analysis results for concrete mixes considered in the analytical study.

5. Conclusions

- Based on the TGA results, the concretes with RHA experienced a greater mass drop than those without RHA at temperatures from 200 to 300. This can be attributed to the fact that incorporating 5% RHA in CACC increases the hydration level and in turn improves the mechanical features compared with the concrete without RHA at an age of 90 days.
- All the mechanical features of the 90-day specimens were higher than those of the 7- and 28-day specimens. Furthermore, at 90 days, the specimens with RHA had higher mechanical features than the control specimens, and the specimen with 5% RHA had the maximum improvement. The reason for this is a higher hydration level in concrete containing RHA, which led to a larger loss of mass in the 200–300 °C range in the TGA test, as a result of the C-S-H gel degradation.
- The recipe midpoint and endpoint methods were used to assess the environmental impacts and the results showed the positive environmental impacts of using RHA in concrete. In this regard, adding 5 and 10% RHA in concrete decreased CO₂ emissions by 18.75% and 38%, fine particulate matter release by 34% and 68%, and ozone depletion level by 31% and 60%, respectively. Critical environmental aspects including CO₂ emissions, fine particulate matter release, ozone depletion, and land use notably decreased by replacing cement with RHA.

Author Contributions: Conceptualization, A.A.; methodology, A.A.; software, A.A.; validation, A.A. and B.S.; formal analysis, A.A. and F.A.; investigation, A.A. and F.A.; resources, A.A. and F.A.; data curation, A.A.; writing—original draft preparation, A.A.; writing—review and editing, B.S. and F.A.; visualization, A.A.; supervision, B.S.; project administration, A.A.; funding acquisition, B.S. All authors have read and agreed to the published version of the manuscript.

Funding: This research received no external funding.

Conflicts of Interest: The authors declare no conflict of interest.

References

1. Jefferis, S.A.; Mangabhai, R.J. Effect of temperature rise on properties of high alumina cement grout. In *Calcium Aluminate Cements*; Chapman and Hall: London, UK, 1990; p. 363.
2. Scrivener, K.L.; Cabiron, J.-L.; Letourneux, R. High-performance concretes from calcium aluminate cements. *Cem. Concr. Res.* **1999**, *29*, 1215–1223. [\[CrossRef\]](#)
3. Bensted, J. Calcium aluminate cements. *Struct. Perform. Cem.* **2002**, *2*, 114–138.
4. Parr, C.; Wöhrmeyer, C.; Veyrat, D. High purity calcium aluminate binders for demanding high temperature applications. In Proceedings of the centenary conference “Calcium Aluminate Cements”, Avignon, France, 30 June–2 July 2008; pp. 417–428.
5. Williams, C.M.; Garrott, F. Recycling/Reclaiming a savings spree: Chicago reuses to the max on famous shopping mile. *Ill. Interchang. Ill. Dep. Transp. Springf.* **2012**. Available online: <https://www.roadbridges.com/recyclingreclaiming-savings-spre> (accessed on 5 January 2022).
6. Abolhasani, A.; Nazarpour, H.; Dehestani, M. The fracture behavior and microstructure of calcium aluminate cement concrete with various water-cement ratios. *Theor. Appl. Fract. Mech.* **2020**, *109*, 102690. [\[CrossRef\]](#)
7. Scrivener, K.L.; Taylor, H.F.W. Microstructural development in pastes of a calcium aluminate cement. In *Calcium Aluminate Cements*; Mangabhai, R.J., Ed.; 1990; Available online: https://www.researchgate.net/publication/40754958_Microstructural_development_of_calcium_aluminate_cement_based_systems_with_and_without_supplementary_cementitious_materials (accessed on 5 January 2022).
8. Abolhasani, A.; Samali, B.; Aslani, F. Physicochemical, Mineralogical, and Mechanical Properties of Calcium Aluminate Cement Concrete Exposed to Elevated Temperatures. *Materials* **2021**, *14*, 3855. [\[CrossRef\]](#) [\[PubMed\]](#)
9. Khaliq, W.; Khan, H.A. High temperature material properties of calcium aluminate cement concrete. *Constr. Build. Mater.* **2015**, *94*, 475–487. [\[CrossRef\]](#)
10. Antonovič, V.; Kerienė, J.; Boris, R.; Aleknevičius, M. The Effect of Temperature on the Formation of the Hydrated Calcium Aluminate Cement Structure. *Procedia Eng.* **2013**, *57*, 99–106. [\[CrossRef\]](#)
11. Newman, J.; Choo, B.S. *Advanced Concrete Technology Set*; Elsevier: Amsterdam, The Netherlands, 2003.
12. Bronzeoak Ltd. Rice Husk Ash Market Study. Available online: www.berr.gov.uk/files/file15138.pdf (accessed on 5 January 2022).
13. Rizwan, S.A. High-Performance Mortars and Concretes Using Secondary Raw Materials. Ph.D. Thesis, Technischen Universitat Bergakademie, Freiberg, Germany, 2006.
14. Kamiya, K.; Oka, A.; Nasu, H.; Hashimoto, T. Comparative Study of Structure of Silica Gels from Different Sources. *J. Sol-Gel Sci. Technol.* **2000**, *19*, 495–499. [\[CrossRef\]](#)
15. Mehta, P.K. Rice husk ash—A unique supplementary cementing material. In *Proceeding International Symposium on Advances in Concrete Technology*; Malhotra, V.M., Ed.; Symposium Paper: Athens, Greece, 1992; pp. 407–430.
16. Della, V.P.; Kühn, I.; Hotza, D. Rice husk ash as an alternate source for active silica production. *Mater. Lett.* **2002**, *57*, 818–821. [\[CrossRef\]](#)
17. Henry, C.S.; Lynam, J.G. Embodied energy of rice husk ash for sustainable cement production. *Case Stud. Chem. Environ. Eng.* **2020**, *2*, 100004. [\[CrossRef\]](#)
18. Mehta, P.K. Role of pozzolanic and cementitious material in sustainable development of the concrete industry. *Int. Concr. Abstr. Portal* **1998**, *178*, 1–20.
19. Ganesan, K.; Rajagopal, K.; Thangavel, K. Rice husk ash blended cement: Assessment of optimal level of replacement for strength and permeability properties of concrete. *Constr. Build. Mater.* **2008**, *22*, 1675–1683. [\[CrossRef\]](#)
20. El-Dakroury, A.; Gasser, M.S. Rice husk ash (RHA) as cement admixture for immobilization of liquid radioactive waste at different temperatures. *J. Nucl. Mater.* **2008**, *381*, 271–277. [\[CrossRef\]](#)
21. Feng, Q.; Yamamichi, H.; Shoya, M.; Sugita, S. Study on the pozzolanic properties of rice husk ash by hydrochloric acid pre-treatment. *Cem. Concr. Res.* **2004**, *34*, 521–526. [\[CrossRef\]](#)
22. Burritt, R.L.; Herzig, C.; Tadeo, B.D. Environmental management accounting for cleaner production: The case of a Philippine rice mill. *J. Clean. Prod.* **2009**, *17*, 431–439. [\[CrossRef\]](#)
23. Alnahhal, M.F.; Alengaram, U.J.; Jumaat, M.Z.; Alqedra, M.A.; Mo, K.H.; Sumesh, M. Evaluation of Industrial By-Products as Sustainable Pozzolanic Materials in Recycled Aggregate Concrete. *Sustainability* **2017**, *9*, 767. [\[CrossRef\]](#)
24. Limbachiya, M.; Meddah, M.S.; Ouchagour, Y. Use of recycled concrete aggregate in fly-ash concrete. *Constr. Build. Mater.* **2012**, *14*, 13–18. [\[CrossRef\]](#)
25. Abolhasani, A.; Aslani, F.; Samali, B.; Ghaffar, S.H.; Fallahnejad, H.; Banihashemi, S. Silicate impurities incorporation in calcium aluminate cement concrete: Mechanical and microstructural assessment. *Adv. Appl. Ceram.* **2021**, *120*, 104–116. [\[CrossRef\]](#)
26. Abolhasani, A.; Shakouri, M.; Dehestani, M.; Samali, B.; Banihashemi, S. A comprehensive evaluation of fracture toughness, fracture energy, flexural strength and microstructure of calcium aluminate cement concrete exposed to high temperatures. *Eng. Fract. Mech.* **2022**, *261*, 108221. [\[CrossRef\]](#)
27. Abolhasani, A.; Nazarpour, H.; Dehestani, M. Effects of silicate impurities on fracture behavior and microstructure of calcium aluminate cement concrete. *Eng. Fract. Mech.* **2020**, *242*, 107446. [\[CrossRef\]](#)
28. Abolhasani, A.; Samali, B.; Dehestani, M.; Libre, N.A. Effect of rice husk ash on mechanical properties, fracture energy, brittleness and aging of calcium aluminate cement concrete. *Structures* **2021**, *36*, 140–152. [\[CrossRef\]](#)

29. Kurda, R.; Silvestre, J.D.; de Brito, J. Life cycle assessment of concrete made with high volume of recycled concrete aggregates and fly ash. *Resour. Conserv. Recycl.* **2018**, *139*, 407–417. [CrossRef]
30. Jiang, M.; Chen, X.; Rajabipour, F.; Hendrickson, C.T. Comparative Life Cycle Assessment of Conventional, Glass Powder, and Alkali-Activated Slag Concrete and Mortar. *J. Infrastruct. Syst.* **2014**, *20*, 04014020. [CrossRef]
31. Robayo-Salazar, R.; Mejia-Arcila, J.; de Gutiérrez, R.M.; Martínez, E. Life cycle assessment (LCA) of an alkali-activated binary concrete based on natural volcanic pozzolan: A comparative analysis to OPC concrete. *Constr. Build. Mater.* **2018**, *176*, 103–111. [CrossRef]
32. Vayghan, A.G.; Khaloo, A.R.; Nasiri, S.; Rajabipour, F. Studies on the Effect of Retention Time of Rice Husk Combustion on the Ash's Chemo-Physical Properties and Performance in Cement Mixtures. *J. Mater. Civ. Eng.* **2012**, *24*, 691–697. [CrossRef]
33. Chao-Lung, H.; Tuan, B.L.A.; Chun-Tsun, C. Effect of rice husk ash on the strength and durability characteristics of concrete. *Constr. Build. Mater.* **2011**, *25*, 3768–3772. [CrossRef]
34. Madandoust, R.; Ranjbar, M.M.; Moghadam, H.A.; Mousavi, S.Y. Mechanical properties and durability assessment of rice husk ash concrete. *Biosyst. Eng.* **2011**, *110*, 144–152. [CrossRef]
35. American Standard Testing and Material. Standard Specification for Concrete Aggregates. 2003. Available online: <https://www.studocu.com/row/document/rajanagarindra-rajabhat-university/marketing-communication/c-33-03-standard-specification-for-concrete-aggregates/8672282> (accessed on 5 January 2022).
36. BS EN 12390-3. Testing Hardened Concrete. Method of Determination of Compressive Strength of Concrete Cubes. 2000. Available online: [http://www.engr.hk/T06/BS%20EN%2012390-3\(2002\).pdf](http://www.engr.hk/T06/BS%20EN%2012390-3(2002).pdf) (accessed on 5 January 2022).
37. ASTM. Standard Test Method for Splitting Tensile Strength of Cylindrical Concrete Specimens. C496/C496M-11. 2011. Available online: <https://pdfcoffee.com/standard-test-method-for-splitting-tensile-strength-of-cylindrical-concrete-specimens-1-pdf-free.html> (accessed on 5 January 2022).
38. Zobel, T.; Almroth, C.; Bresky, J.; Burman, J.-O. Identification and assessment of environmental aspects in an EMS context: An approach to a new reproducible method based on LCA methodology. *J. Clean. Prod.* **2002**, *10*, 381–396. [CrossRef]
39. ISO. Environmental Management: Life Cycle Assessment. In *Principles and Framework*; ISO: Geneva, Switzerland, 2006; Volume 14044.
40. Schneider, L.; Berger, M.; Finkbeiner, M. The anthropogenic stock extended abiotic depletion potential (AADP) as a new parameterisation to model the depletion of abiotic resources. *Int. J. Life Cycle Assess.* **2011**, *16*, 929–936. [CrossRef]
41. Junnila, S.; Horvath, A.; Guggemos, A.A. Life-Cycle Assessment of Office Buildings in Europe and the United States. *J. Infrastruct. Syst.* **2006**, *12*, 10–17. [CrossRef]
42. Khasreen, M.M.; Banfill, P.F.G.; Menzies, G.F. Life-Cycle Assessment and the Environmental Impact of Buildings: A Review. *Sustainability* **2009**, *1*, 674–701. [CrossRef]
43. ISO. *Internationale de Normalisation, Sustainability in Building Construction: Environmental Declaration of Building Products*; ISO: Geneva, Switzerland, 2007.
44. AzariJafari, H.; Amiri, M.J.T.; Ashrafi, A.; Rasekh, H.; Barforooshi, M.J.; Berenjian, J. Ternary blended cement: An eco-friendly alternative to improve resistivity of high-performance self-consolidating concrete against elevated temperature. *J. Clean. Prod.* **2019**, *223*, 575–586. [CrossRef]
45. Chungsangunsit, T. Environmental Assessment of Electricity Production from Rice Husk: A Case Study in Thailand, Electricity Supply Industry in Transition: Issues and Prospect for Asia. EU-ASEAN COGEN 3 Program. 2004. Available online: <https://books.google.com/books?id=eHENDgAAQBAJ&pg=PA184&lpg=PA184&dq=Environmental+Assessment+of+Electricity+Production+from+Rice+Husk:+A+Case+Study+in+Thailand,+Electricity+Supply+Industry+in+Transition:+Issues+and+Prospect+for+Asia&source=bl&ots=naLV5av-ud&sig=ACfU3U0R3EeUbk1BPq7slm01Tk0khqEZQ&hl=id&sa=X&ved=2ahUKEwiWie3vj7j1AhVKZt4KHUo1AooQ6AF6BagCEAM#v=onepage&q=Environmental%20Assessment%20of%20Electricity%20Production%20from%20Rice%20Husk%3A%20A%20Case%20Study%20in%20Thailand%2C%20Electricity%20Supply%20Industry%20in%20Transition%3A%20Issues%20and%20Prospect%20for%20Asia&f=false> (accessed on 5 January 2022).
46. Wang, Q.; Maezono, T.; Apaer, P.; Chen, Q.; Gui, L.; Itoh, K.; Kurokawa, H.; Sekiguchi, K.; Sugiyama, K.; Niida, H.; et al. Characterization of suspended particulate matter emitted from waste rice husk as biomass fuel under different combustion conditions. *WIT Trans. Ecol. Environ.* **2012**, *157*, 365–376. [CrossRef]
47. Mehta, P.K.; Monteiro, P.J.M. Microstructure and properties of hardened concrete. *Concr. Microstruct. Prop. Mater.* **2006**, 41–80.
48. Padhi, R.S.; Patra, R.K.; Mukharjee, B.B.; Dey, T. Influence of incorporation of rice husk ash and coarse recycled concrete aggregates on properties of concrete. *Constr. Build. Mater.* **2018**, *173*, 289–297. [CrossRef]
49. Chindaprasirt, P.; Homwuttiwong, S.; Jaturapitakkul, C. Strength and water permeability of concrete containing palm oil fuel ash and rice husk-bark ash. *Constr. Build. Mater.* **2007**, *21*, 1492–1499. [CrossRef]
50. Le, H.T.; Nguyen, S.T.; Ludwig, H.-M. A Study on High Performance Fine-Grained Concrete Containing Rice Husk Ash. *Int. J. Concr. Struct. Mater.* **2014**, *8*, 301–307. [CrossRef]
51. Thomas, B.S.; Gupta, R.C.; Kalla, P.; Csetenyi, L. Strength, abrasion and permeation characteristics of cement concrete containing discarded rubber fine aggregates. *Constr. Build. Mater.* **2014**, *59*, 204–212. [CrossRef]
52. Noaman, M.A.; Islam, M.N.; Islam, M.R.; Karim, M.R. Mechanical properties of brick aggregate concrete containing rice husk ash as a partial replacement of cement. *J. Mater. Civ. Eng.* **2018**, *30*, 4018086. [CrossRef]

-
53. Salas, A.; Delvasto, S.; DE Gutierrez, R.M.; Lange, D. Comparison of two processes for treating rice husk ash for use in high performance concrete. *Cem. Concr. Res.* **2009**, *39*, 773–778. [[CrossRef](#)]
 54. Van Tuan, N.; Ye, G.; van Breugel, K.; Fraaij, A.L.; Bui, D.D. The study of using rice husk ash to produce ultra high performance concrete. *Constr. Build. Mater.* **2011**, *25*, 2030–2035. [[CrossRef](#)]
 55. Fapohunda, A.C.; Akinbile, B.; Shittu, A. Structure and properties of mortar and concrete with rice husk ash as partial replacement of ordinary Portland cement—A review. *Int. J. Sustain. Built Environ.* **2017**, *6*, 675–692. [[CrossRef](#)]
 56. Nazari, A.; Riahi, S. RETRACTED: Splitting tensile strength of concrete using ground granulated blast furnace slag and SiO₂ nanoparticles as binder. *Energy Build.* **2011**, *43*, 864–872. [[CrossRef](#)]